X-692-70-89
PREPRINT
NASA TM X- 63856

MAGNETIC POTENTIAL MODEL FOR THE STRUCTURE OF THE SOLAR CORONA FOR THE MARCH 1970 ECLIPSE

K. H. SCHATTEN

MARCH 1970

GSFC — GODDARD SPACE FLIGHT CENTER
GREENBELT MARYLAND

X-692-70-89

MAGNETIC POTENTIAL MODEL FOR THE STRUCTURE OF THE SOLAR CORONA FOR THE MARCH 1970 ECLIPSE*

K. H. Schatten
Laboratory for Extraterrestrial Physics
NASA-Goddard Space Flight Center
Greenbelt, Maryland

March 1970

*Invited lecture presented March 6, 1970 at the Solar Eclipse Conference, East Carolina University, Greenville, North Carolina

Abstract

Features of the solar corona observable at the time of a solar eclipse are discussed and compared with ground based measurements of the corona using a standard coronagraph. A model for determining the large scale structure of the coronal and interplanetary magnetic fields is presented. The effects of solar activity upon the model and the observed corona are shown. The application of the model to observable features of the solar corona at the time of solar eclipses is discussed. In particular the recent Siberian solar eclipse is compared with predictions from the model. The features expected from the model for the March 1970 solar eclipse are shown.

In discussing solar eclipse phenomena it is valuable to compare what information may be obtained using coronagraph measurements during ordinary daylight conditions. Concerning this matter, considerations will be restricted to the visible portion of the spectrum.

At the time of a solar eclipse the sun's atmosphere becomes visible. Figure 1 from Zirin (1966) shows the relative intensity of various features present in coronal light as a function of radial distance from the sun.

The K corona represents the electronic (or plasma) component of the sun's atmosphere. It can be seen that its brightness is about one millionth that of the sun and is the predominant intensity component of the sun's visible radiation spectrum emanating from regions 1 to $2\frac{1}{4}$ solar radii, at which point the F coronal intensity predominates. This region represents the inner zodiacal light (or interplanetary dust component) of the corona. Thus, beyond about 2.5 solar radii it becomes difficult to photograph the K corona at the time of a solar eclipse. The fact that the skylight intensity is comparable with and in most cases greater than the coronal light intensity prevents ordinary daylight coronal observations without the use of a coronagraph. This instrument, a typical example of which is shown in Figure 2, allows only a small portion of the spectrum to be observed. As a result the portion of the spectrum with the greatest intensity, the emission lines of ions, can only be observed by filtering out most of the skylight not in their spectral range. This, however, allows only the E (or emission) corona to be observed.

Using the coronagraph one can observe three classes of emission lines; the low, medium, and high excitation lines. The classifications refer to the amount of solar activity. They can be seen at various position angles about the sun but at the expense of resolution and even then only for a few tenths of a solar radius above the photosphere. Thus, one might be able to tell the position of a bright feature or of a region of high activity by studying these emission lines. However, not much topological information concerning coronal structure can be derived in this manner. Ordinarily the red and green lines of Fe XV (6374Å) and Fe-IV (5303Å) are monitored. These are low and medium excitation lines.

Figure 3 shows a photograph of the September 22, 1968, total solar eclipse over the Union of Soviet Socialist Republics and a portion of Western China obtained by Laffineur, Burnichon, and Koutchmy. It is evident that coronal features may be seen in great detail by carefully examining such photographs. The features include a variety of interesting streamers, prominences, and coronal arches.

Figure 4 is a drawing of the 1941 corona according to Bugoslavskaya. This lady solar physicist examined 14 eclipses and identified and classified coronal features in four groups: rays, systems of arches and envelopes above sunspots, systems of arches over prominences, and systems embracing the arches of helmet - like envelopes. This drawing makes clear the great amount of detail that may be obtained about the structure of the corona from eclipse work.

A physical model that is consistent with many of the properties observed in the corona and in interplanetary space has been developed by Schatten et al. (1969). Altschuler and Newkirk (1969) have developed a similar model. This model is an attempt to account for the important effects that the magnetic field has upon the inner corona and the plasma located there. Figure 5 shows a representation of the model.

There are three distinct regions in the model where different physical phenomena occur. Region 1 represents the photosphere, where the magnetic field motion is governed by the detailed motions of the plasma near the photosphere. Above the photosphere the plasma density diminishes very rapidly with only moderate decreases in the magnetic energy density. This results in region 2, where the magnetic energy density is greater than the plasma energy density and hence controls the configuration. We may then utilize the force-free condition, $\vec{j} \times \vec{B} = 0$, and in fact make the more restrictive assumption that region 2 is current free. The magnetic field in region 2 may then be derived from a potential that obeys Laplace's equation: $\nabla^2\varphi = 0$. The scalar potential may then be employed in the solution of the magnetic field configuration in this region. Using the less restrictive force-free condition would allow a 'twisting' of field lines or filamentary structure without substantially changing the large-scale magnetic structure.

Substantially further out in the corona the total magnetic energy density diminishes to a value less than the plasma energy density, and the magnetic field can then no longer structure the solar wind flow.

The magnetic field has, however, become oriented very much in the radial direction, as suggested by Davis (1965). Thus, before the total magnetic energy density falls below the plasma energy density, a region is reached where the transverse magnetic energy density does so. It is the transverse magnetic field that interacts with the coronal plasma, since a radial magnetic field would neither affect nor be affected by a radially flowing plasma. Regions 2 and 3 are separated by the surface where the transverse magnetic energy density falls below the plasma energy density. In region 3 transverse magnetic fields are transported by the radially flowing plasma, and cannot exist in a quasi-static fashion. The magnetic field existing on the surface boundary between regions 2 and 3 is thus oriented in approximately the radial direction, and serves as a source for the interplanetary magnetic field. This 'source' surface is the region where currents in the corona cancel the transverse magnetic field. The region may not in fact be a surface but be a few tenths of a solar radius in thickness.

A solution for the magnetic field inside the source surface is now obtained to permit comparisons of the model with observations. The source surface is approximated as a concentric sphere with the radius R_s. Utilization of a scalar potential φ of the form shown in Figure 6 allows the magnetic field to obey the boundary conditions of a radially oriented field on the source surface. The magnetic field at any location above the photosphere and within the source surface is given by $\vec{B}(R_x) = -\vec{\nabla}\varphi$. In particular, the magnetic field evaluated on

the source surface is shown. The currents flowing on the source surface are given by $\vec{J} = (c/4\pi)\nabla \times \vec{B}$. The magnetic field due to the distribution of sources needed to represent actual observations is then calculated for a particular radius R_s. The magnetic fields calculated on the source surface can then be compared with interplanetary observations to determine R_s and to provide a test of the model. There will certainly be differences between the magnetic field on the source surface and the interplanetary field. The regularity of the interplanetary field, however, suggests that much of the ordering of the field near the sun has not been removed during this transport.

At times of moderate solar activity, correlations with interplanetary magnetic fields indicate a source surface radius of 1.6 solar radii. Figure 7 shows a comparison of calculations from the model using photospheric observations from the Mount Wilson Observatory with interplanetary magnetic fields and coronal green line observations. The model appears capable of calculating the interplanetary magnetic field direction. In addition, enhanced coronal green line emission appears to be associated with higher field strength and closed coronal regions. Figure 8 shows a calculation of the magnetic structure of the corona in the plane perpendicular to the earth-sun line. Many features seen are reminiscent of coronal features such as streamers arches and rays.

Figure 9 shows the intermediate active coronas of 1961 and 1952 with a source surface 0.6 solar radii above the photosphere superposed. Most

arches fall within this sphere. Beyond it the structures becomes oriented more nearly radial in accordance with the model. High latitude streamers can be seen above centers of activity. The streamers and arches appear similar to the features in Figure 8.

The top portion of Figure 10 shows the corona at sunspot minimum on June 30, 1954. The long equatorial streamers and polar plumes are typical of solar minimum. In the bottom of Figure 10 is a description of the magnetic field that would result if equal and opposite polar fields were employed in the source surface model with no equatorial magnetic activity. The general structure of the magnetic field is similar to the structures evident in the eclipse drawing. Thus, the model shows agreement with eclipse observations of the corona at various stages of the solar cycle.

The structure of the corona has been predicted for the September 22, 1968, solar eclipse which had a path of totality over the Union of Soviet Socialist Republics and China, by Schatten (1968). Observations of the eclipse appear to support certain features of the model as described by Schatten (1969) and Laffineur, et al.(1969). Figure 11 (top) shows a sketch of the corona prepared by Professor M. Waldmeier. The bottom portion of the figure is the prediction prepared on September 20, 1968.

No prediction near the poles was made because observations of the photospheric magnetic field are of low quality in these regions. Proceeding counterclockwise from the north pole one can note a variety of similarities between the two figures. In the northeast quadrant, an open-rayed

structure is predicted and observed. The southeast quadrant shows two large helmet-type streamers. Two large streamers are observed. The resolution of the pictures was insufficient, however, to capture enough detail to trace any closed looped structure that may exist within these streamers. The model that predicts the structure of the streamers does so only as far as 0.6 solar radii above the photosphere. Hence the exact predicted direction of these streamers beyond this distance is somewhat uncertain. Cowling (1969) notes that had the streamers been drawn "more nearly radial, the agreement would have been almost perfect".

Above the southwest limb, one large streamer is predicted and observed. This streamer appears to consist of several coronal arches as predicted. Above the western equator some tight coronal arches are predicted with overlying streamer configurations. The direction and position of the rays in the sketch of Waldmeier is consistent with those of the streamers in the prediction. The rays appearing to emanate from the limb of the sun as seen in the sketch may actually emanate from a configuration of closed loops (J. Pasachoff, private communication), as the prediction shows. Professor Waldmeier (private communication) describes this region as "the second-brightest in the corona, but almost structureless". In the northwest quadrant, an open-rayed configuration at low latitudes and a streamer above a prominence chain at higher latitudes were predicted and observed. The fact that the streamer is closed with the open appearance is attributed to the orientation of the streamer base parallel to a meridian, as was the underlying prominence chain.

Another sketch of the coronal structure is shown in Figure 12 by Serge Koutchmy. Many features in this drawing are similar to those in both the drawing of Waldmeier and the prediction sketch.

Figure 13 shows the structure of the 1970 coronal appearance predicted by Schatten (1970) several days before the solar eclipse. The March 7th eclipse will be interesting, astronomically speaking, because of the closeness of its occurrence to the time of maximum solar activity. Predicted coronal features within 60° of latitude from the solar equator are as follows. Position angle (degrees counterclockwise from north pole) of calculated features listed in approximate order of decreasing brightness and certainty: Bright features (condensations) at 288 degrees and 95 degrees; streamer from 100 to 120 degrees overlying 2 coronal arches at 100 and 110 degrees; helmet streamers (with arches) from 30 to 70 degrees centered on 50 degrees and from 285 to 310 degrees centered on 302 degrees; coronal arches at 75, 292, 278 degrees; broad streamers without arches from 235 to 270 degrees and from 120 to 150 degrees; narrow streamers possibly with greater tangential polarization at 235 and 145 degrees. The corona will probably be somewhat brighter and more flattened to the equator than the 1968 eclipse. There appear to be a greater number of solar active regions at lower latitudes following sunspot maximum. Several large streamers, indicative of an active sun, should be apparent.

Acknowledgements

I would like to acknowledge John Wilcox who helped develop many of the ideas presented and also Robert Howard who has aided in understanding solar magnetism and has provided Mt. Wilson solar magnetic field observations. The help of colleagues at Goddard Space Flight Center is also appreciated.

Photographs and discussions of the 1968 Siberian eclipse were made available by Jay Pasachoff, Serge Koutchmy, and M. Waldmeier.

References

Altschuler, M. and Newkirk, Jr., G., Solar Physics 9, (1969) 131-149.

Bugoslavaskaya, E. Ya., Trud. Gos. Astronom. Inst. in Shternberga, 19 (1950), 3.

Cowling, T. G., The Observatory, 89, (1969), 973, 217-224.

Davis, L., Stellar and Solar Magnetic Fields, (1965), (ed. by R. Lüst) North Holland Publishing Co., Amsterdam.

Laffineur, M., Burnichon, M. L., Koutchmy, S., Nature, 222, (1969), 5192, 461.

Nikolskij, G. M., Astron. Zhurn., 30, (1953), 286.

Schatten, K. H., Nature 220, (1968), 5173, 1211-1213.

Schatten, K. H., Wilcox, J. M., and Ness, N. F., Solar Physics, 6 (1969), 442-455.

Schatten, K. H., Nature, 222, (1969), 652.

Schatten, K. H., submitted to Nature (1970).

Vsekhasvjatsky, S. K., The Solar Corona, (1963), (ed, J. W., Evans), Academic Press, London.

Zirin, H., The Solar Atmosphere, (1966), Blaisdell, Waltham, Ma.

FIGURE CAPTIONS

Figure 1 Relative intensity of the components of coronal light. (The coronagraph adds an instrumented brightness log I= -5. After Zirin, 1966).

Figure 2 The Lyot coronagraph, with a single objective lense. An image of the sun is formed on the occulting disk; removing the photospheric light. Coronal light is reimaged by O2 on the spectrograph slit. The bright diffraction ring, the doubly reflected, and scattered light from the objective lense O1 is removed before O2 by diaphragms. (After Zirin, 1966).

Figure 3 Photograph of the September 22, 1968, solar eclipse observed at Yurgamish, Siberia, obtained by M. Laffineur, M. L. Burnichon, and S. Koutchmy (1968).

Figure 4 Structure of the September 21, 1941, corona according to E. Ya. Bugoslavskaya (1950). Coronal rays and a variety of arches are evident in this drawing.

Figure 5 Schematic representation of the source surface model. The photospheric magnetic field is measured in region 1 at Mount Wilson Observatory. Closed field lines (loops) exist in Region 2. The field in this region is calculated from potential theory. Currents flowing near the source surface eliminate the transverse components of the magnetic

field, and the solar wind extends the source surface magnetic field into interplanetary space. The magnetic field is then observed by spacecraft near 1 AU.

Figure 6 The potential solution for the magnetic field produced by a source of field lines with a normal magnetic field boundary condition is shown. The magnetic field on the source surface $\vec{B}_n$ is also calculated.

Figure 7 Computed magnetic configuration of the inner corona at latitude 15°N for Carrington solar rotation 1495. The interval from June 5, 1965, through July 2, 1965, is included. The source surface is represented by the middle circle with an indication of the Julian day of central meridian passage. The solid lines drawn between the photosphere and the source surface indicate magnetic field lines oriented away from the sun and the dashed lines indicate toward-the-sun magnetic field. Coronal green line (5303Å) intensities are indicated by three different thicknesses of bars drawn inside the inner circle. The radial component of the interplanetary magnetic field is placed on the outermost circle. Solid or dashed lines indicate away or toward-the-sun interplanetary sectors.

Figure 8 Computed configuration of the coronal magnetic field above the limbs of the sun on November 6, 1965.

Figure 9 Drawing of the February 15, 1961, eclipse (Vsekhasvjatsky, 1963) (top). Drawing of the corona during the February 25, 1952, eclipse (Nikolskij, 1953) (bottom).

Figure 10 Drawing of the corona at the June 30, 1954, eclipse near solar minimum (Vsekhsvjatsky, 1963) (top). Appearance of the field line configuration in the corona using the "source surface" model with only polar fields present in the photosphere (bottom).

Figure 11 Sketch of the September 22, 1968, solar eclipse drawn by Professor M. Waldmeier (top). The shaded areas represent streamers. Prediction of the coronal structure drawn on September 20, 1968, (bottom). (After Schatten 1968).

Figure 12 Sketch of the September 22, 1968, solar eclipse drawn by Dr. Serge Koutchmy.

Figure 13 March 7, 1970, solar eclipse prediction from source surface model.

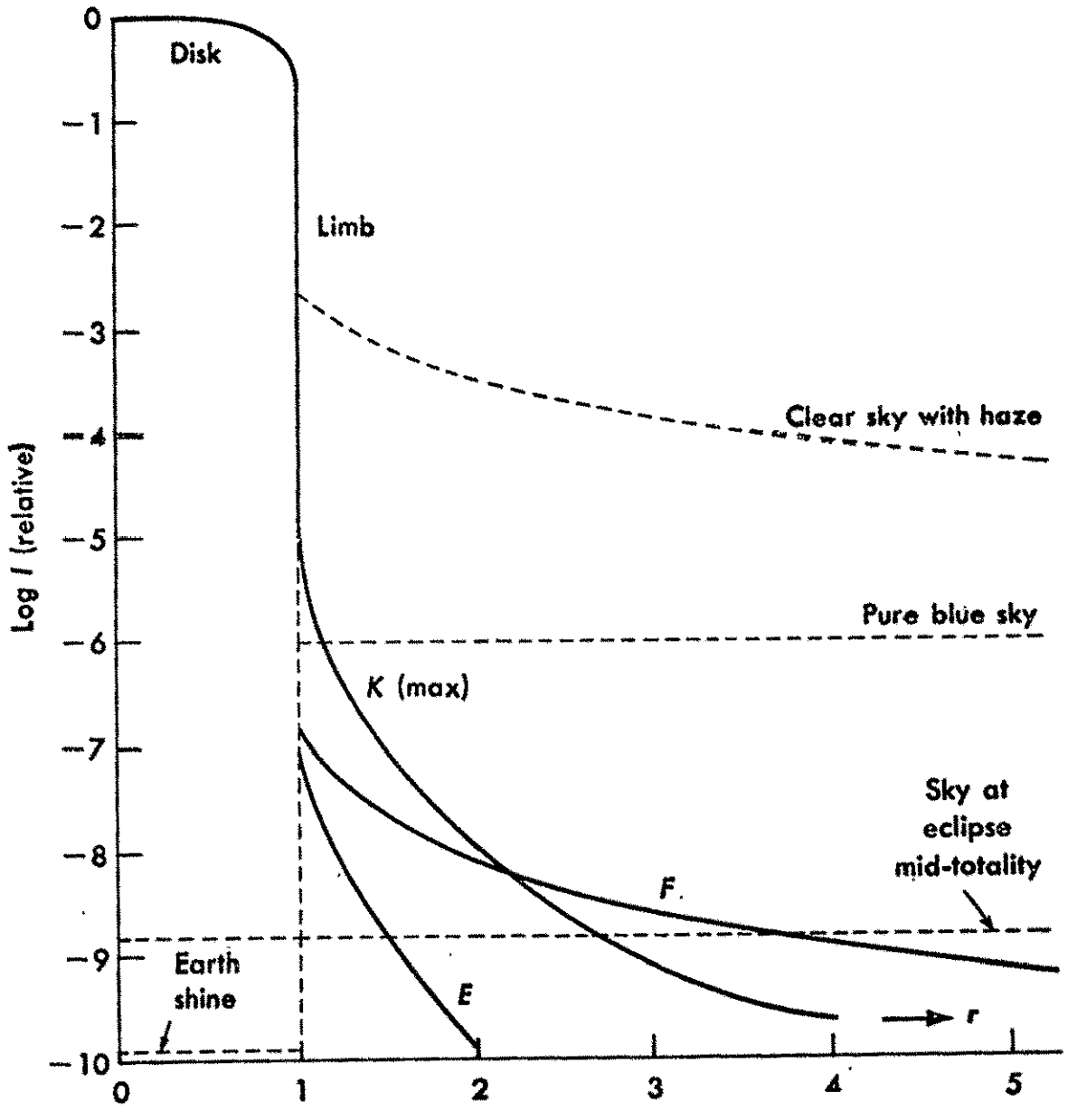
0
−1
−2
−3
−4
−5
−6
−7
−8
−9
−10
Log I (relative)
0
1
2
3
4
5
Disk
Limb
Clear sky with haze
Pure blue sky
K (max)
F
Sky at
eclipse
mid-totality
E
Earth
shine
r

FIGURE 1

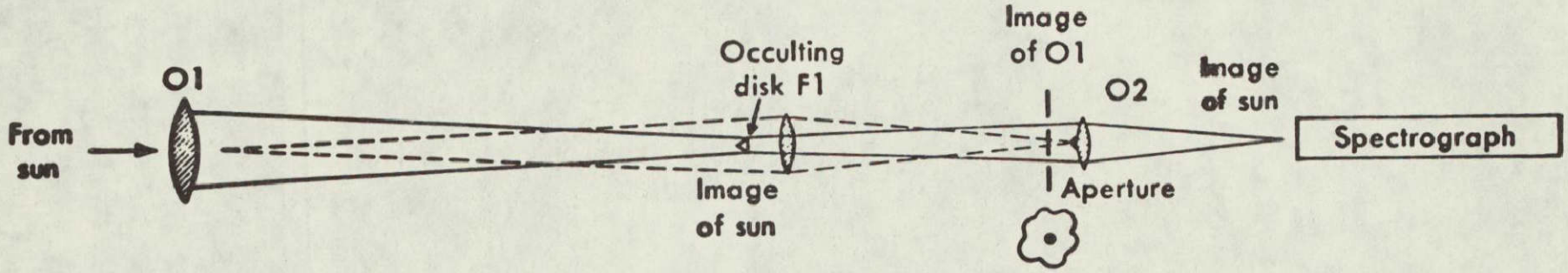
O1
From sun
Occulting disk F1
Image of sun
Image of O1
O2
Image of sun
Spectrograph
Aperture

FIGURE 2

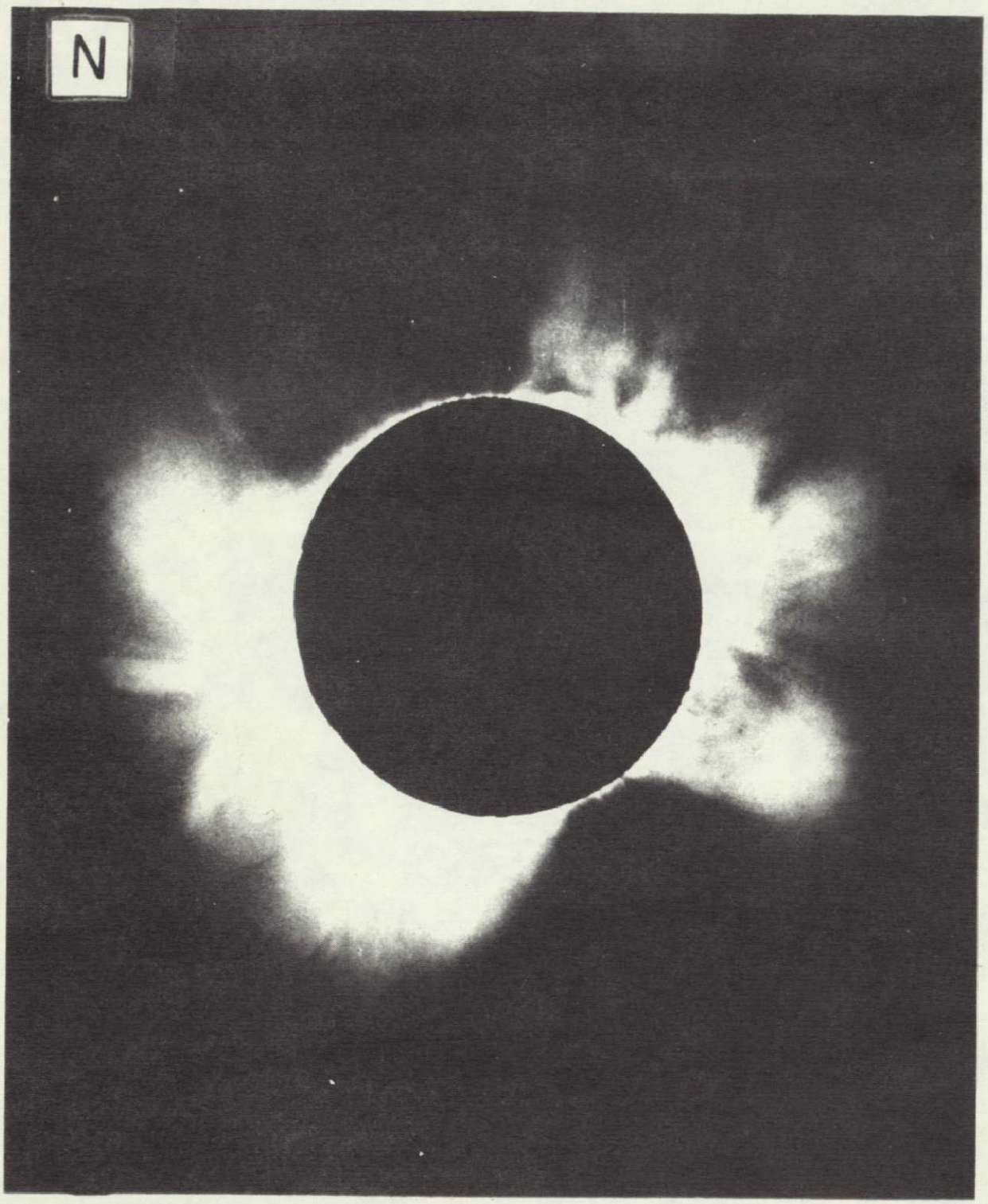

LA COURONNE SOLAIRE DU 22 SEPT 1968 A 11H20 T.U.
Photographie avec atténuation radiale obtenue à Yurgamish (URSS)
Mission Française LAFFINEUR M. BURNICHON M.L. KOUTCHMY S.
Région spectrale 5500-6500 Å environ. Δt=30 sec. F=1526mm.
D= 100 mm. Film Kodak LS Pan 50 ASA

FIGURE 3

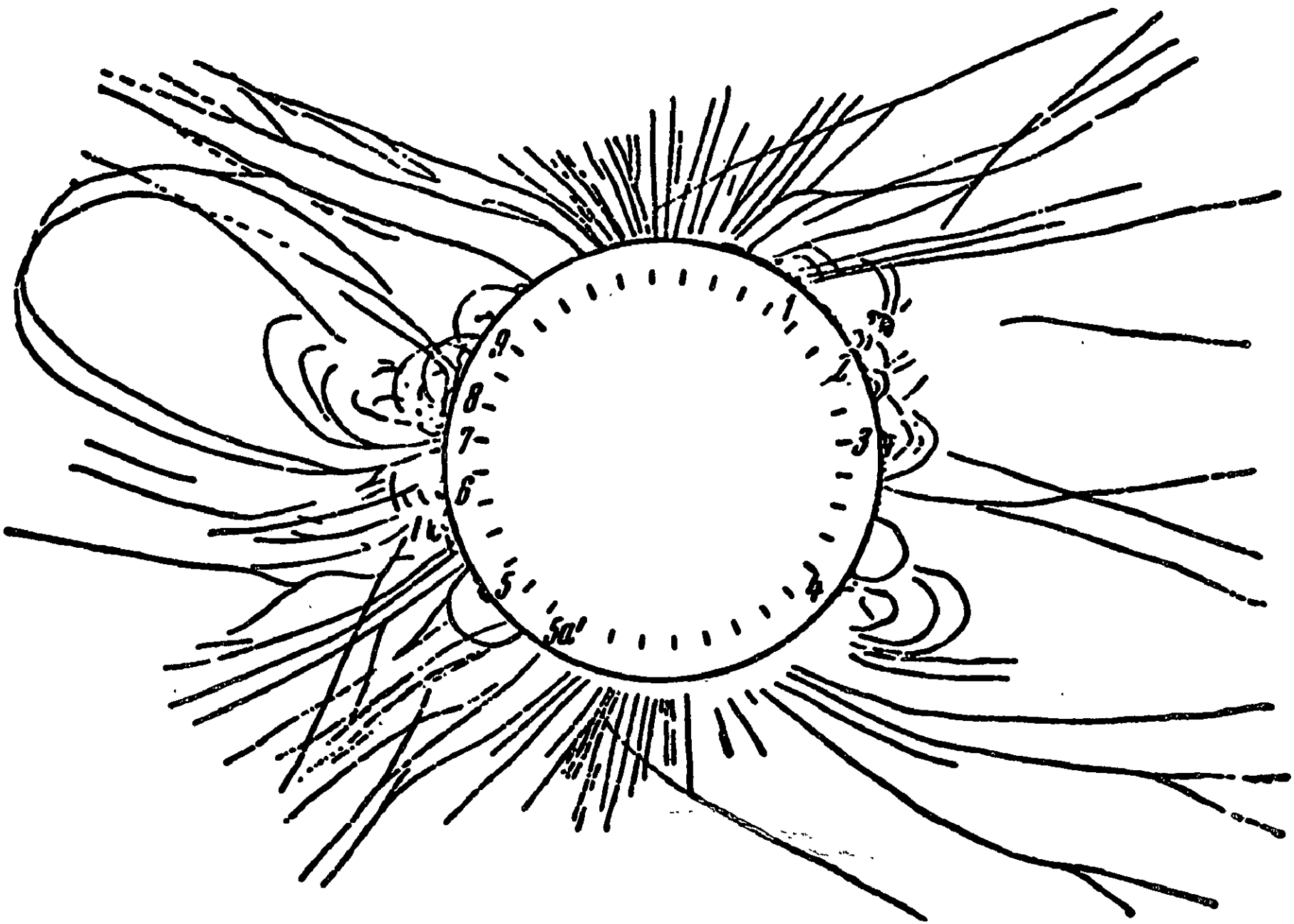

FIGURE 4

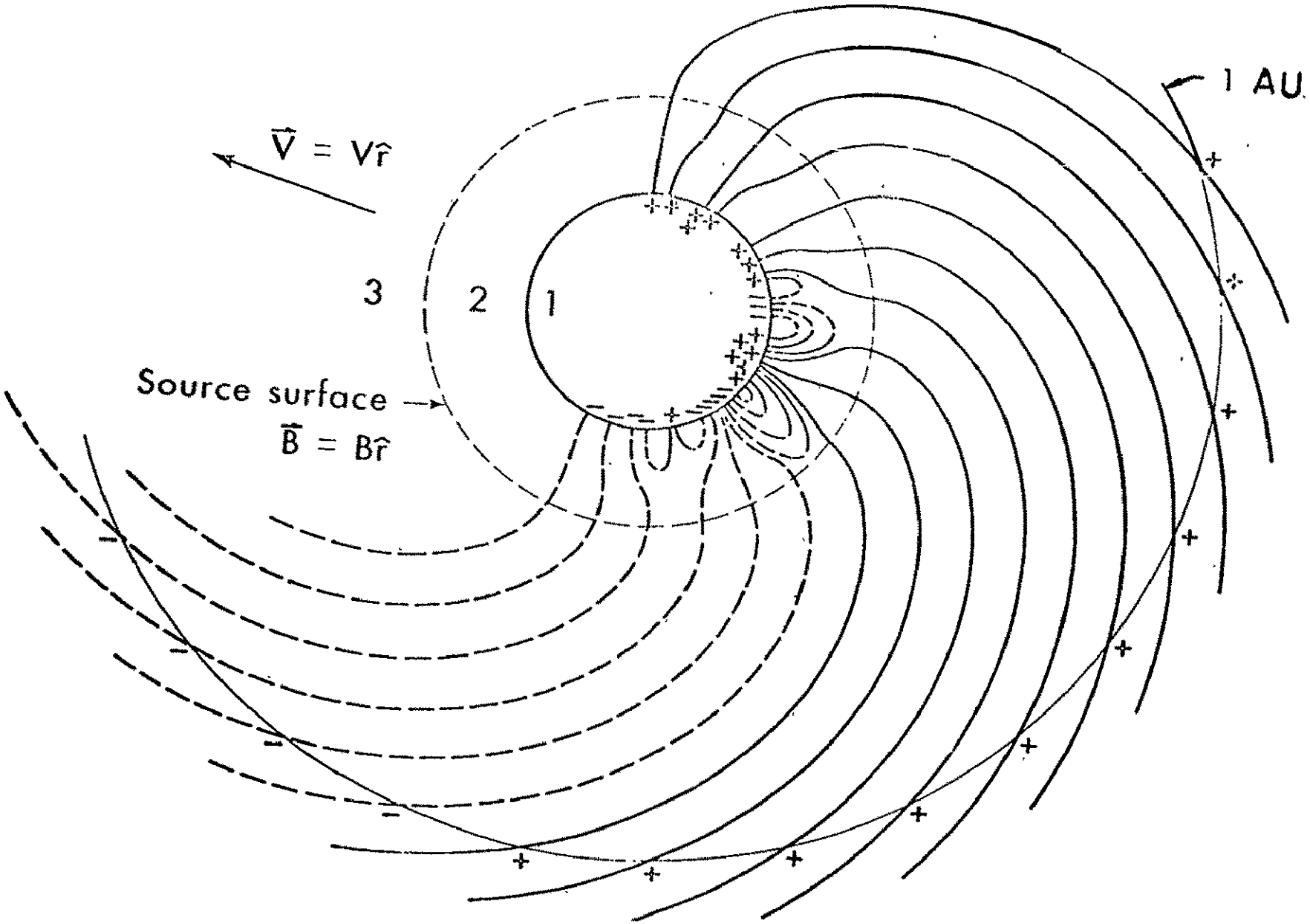

FIGURE 5

GREEN'S FUNCTION SOLUTION OF MAGNETIC FIELD INSIDE SOURCE SURFACE

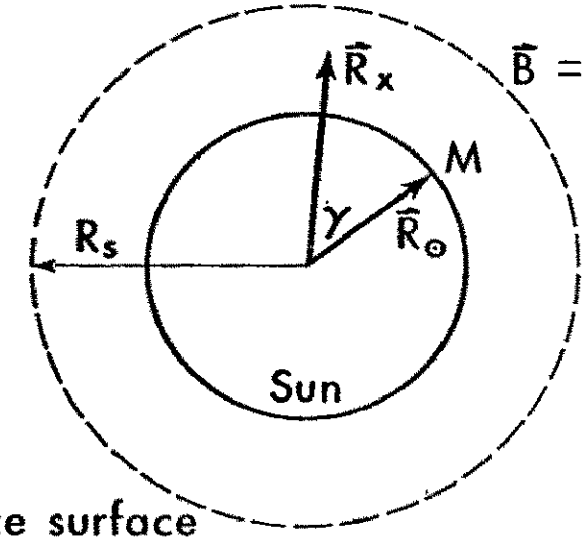

Source surface

Source of field lines of strength M at position $\vec{R}_\odot$ or θ', ϕ' on sun

Potential at $\vec{R}_x$ =

$$\Phi(\vec{R}_x) = \frac{M}{|\vec{R}_x - \vec{R}_\odot|} - \frac{M\,R_s/R_\odot}{|\vec{R}_x - \vec{R}_\odot R_s^2/R_\odot^2|}$$

$$\vec{B}(\vec{R}_x) = -\nabla\Phi$$

Magnetic field due to source M

$$\vec{B}_n = -\frac{M\hat{r}}{R_s^2}\,\frac{R_s}{R_\odot}\left(1-\frac{R_s^2}{R_\odot^2}\right)\Big/\left(1+\frac{R_s^2}{R_\odot^2}-\frac{2R_s}{R_\odot}\cos\gamma\right)^{3/2}$$

Magnetic field due to distribution of sources

$$\vec{B}_n(\theta,\phi;\,R_s) \int \vec{B}_n(\theta,\phi,\theta',\phi';\,R_s)\cdot M(\theta',\phi')\,d\Omega'$$

FIGURE 9

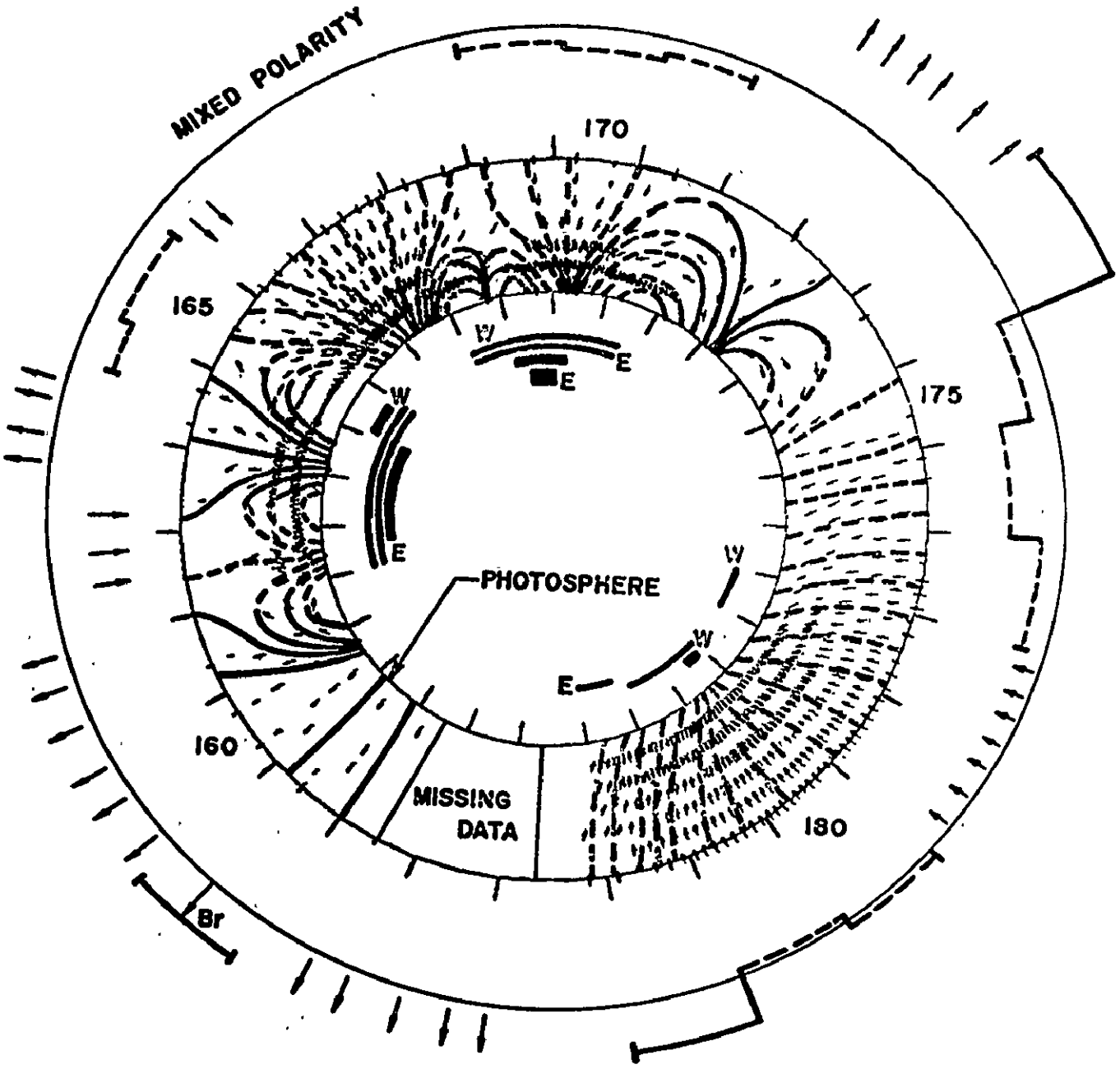
MIXED POLARITY
170
165
175
160
180
W
E
E
W
E
W
PHOTOSPHERE
E
W
MISSING
DATA
Br

FIGURE 7

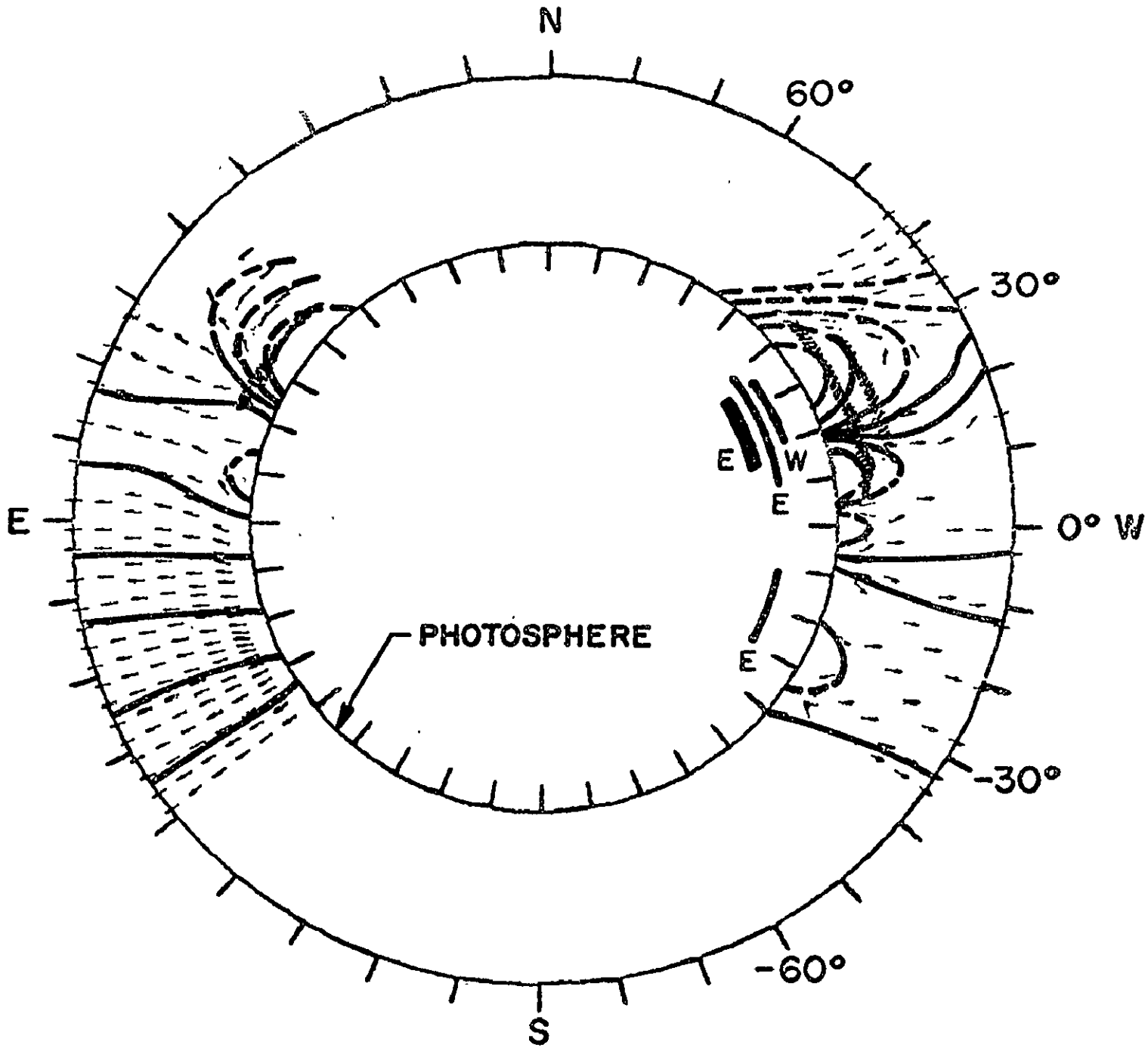

FIGURE 8

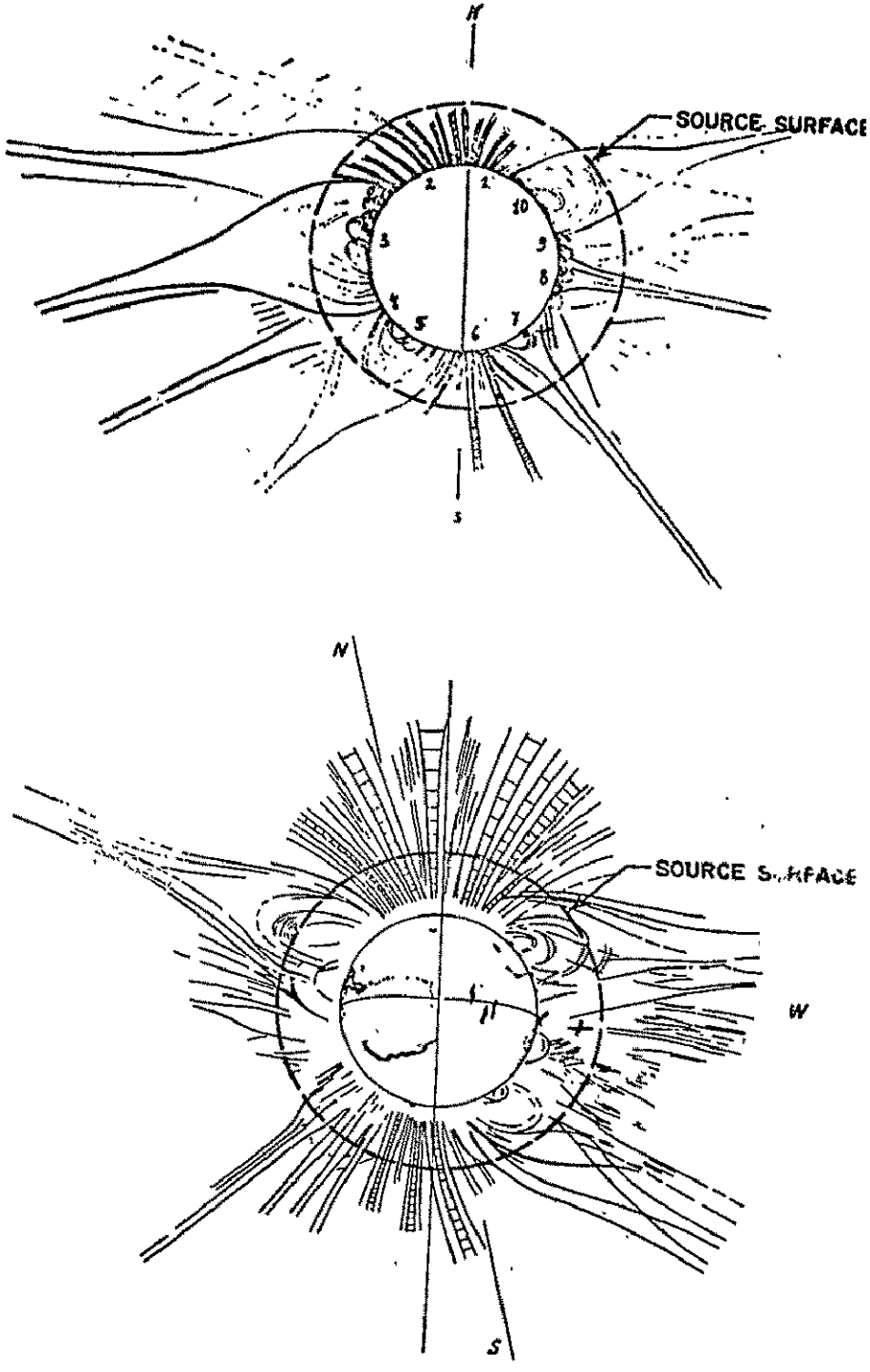

FIGURE 9

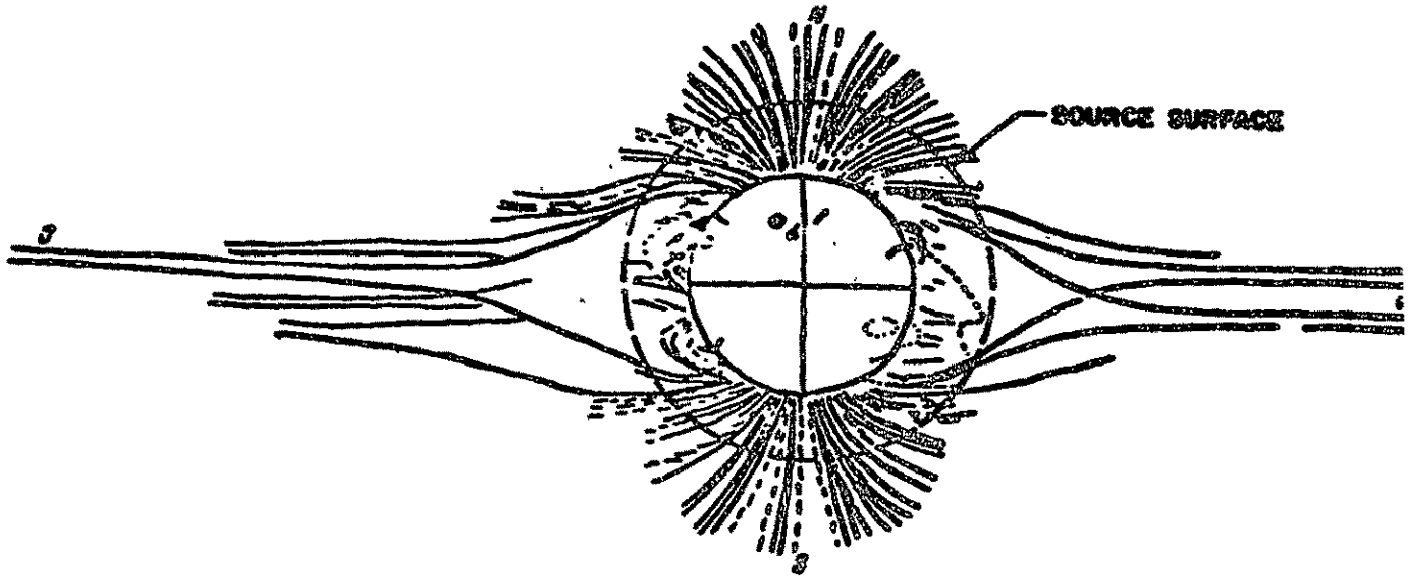

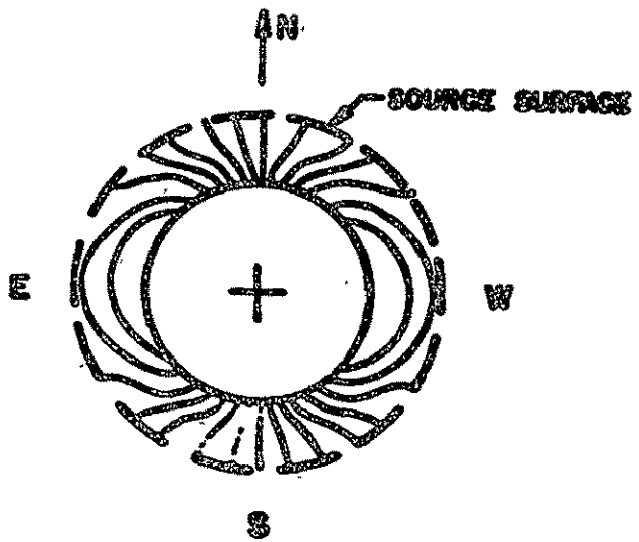

FIGURE

SOLAR ECLIPSE
September 22, 1968

OBSERVATION
(Waldmeier)

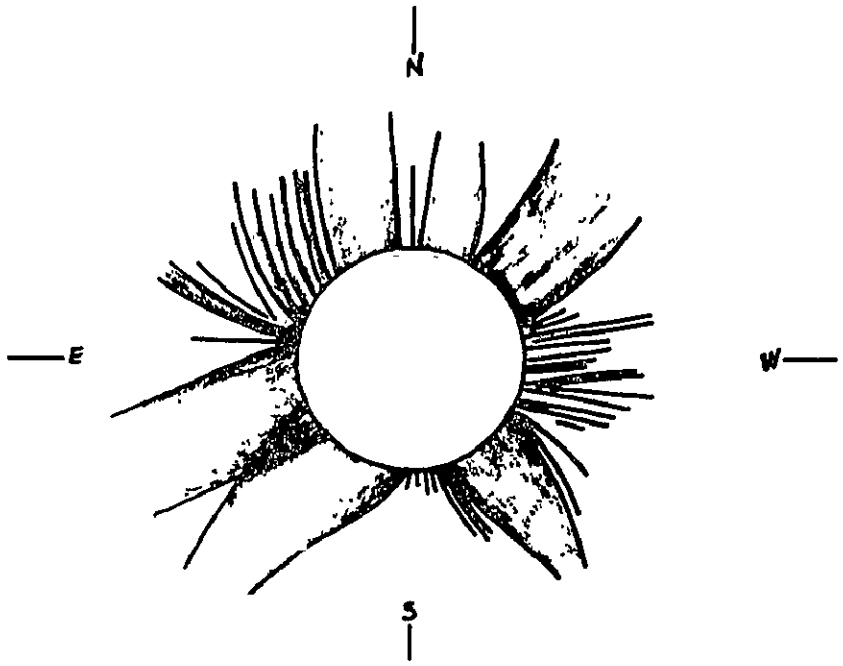

PREDICTION

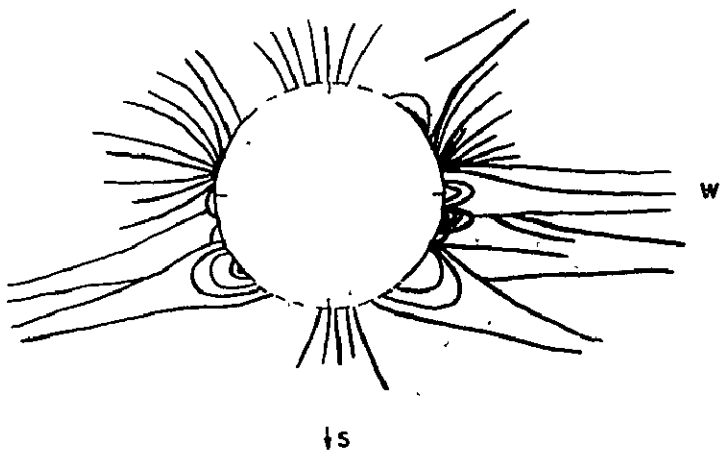

FIGURE 11

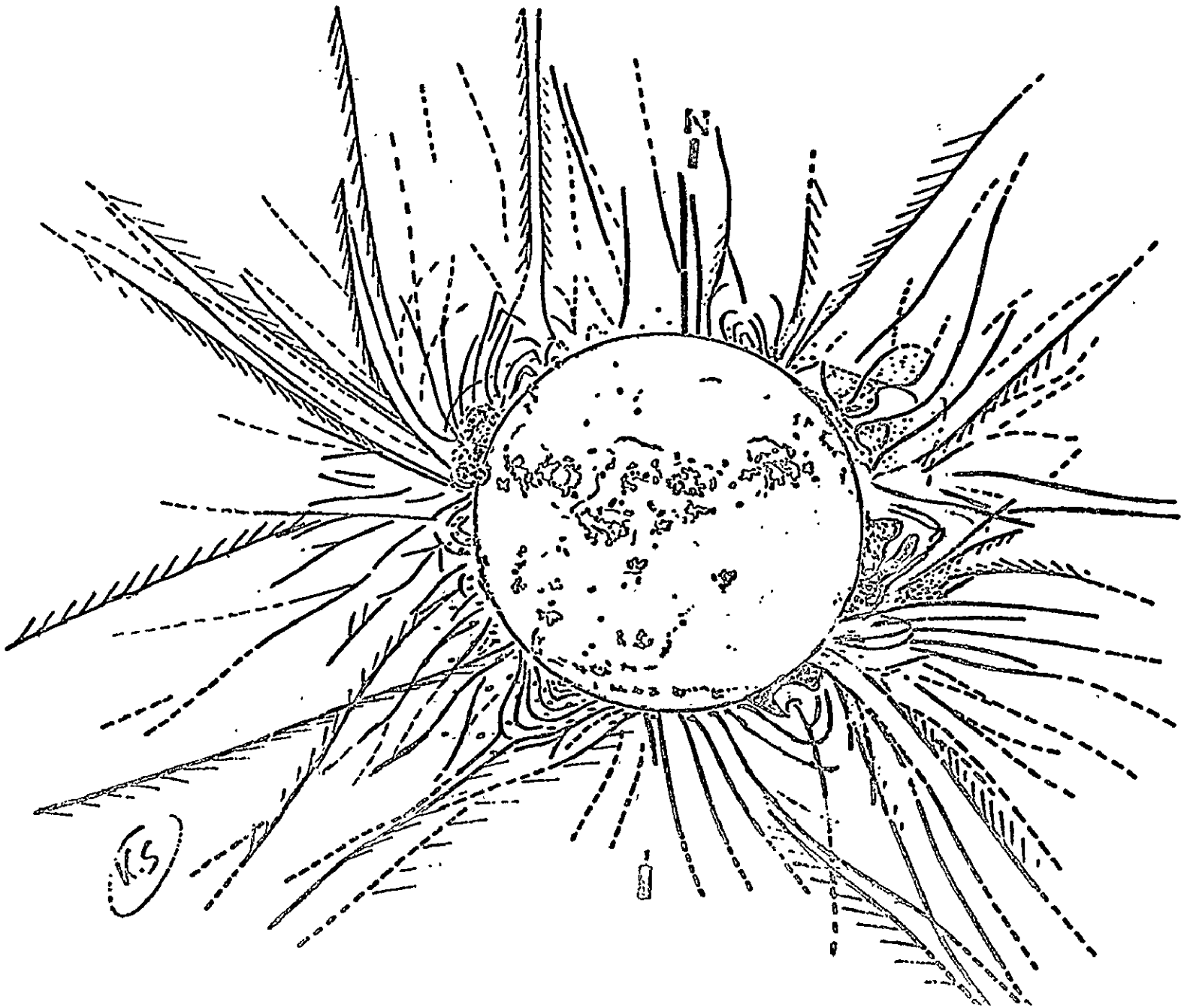

FIGURE 12

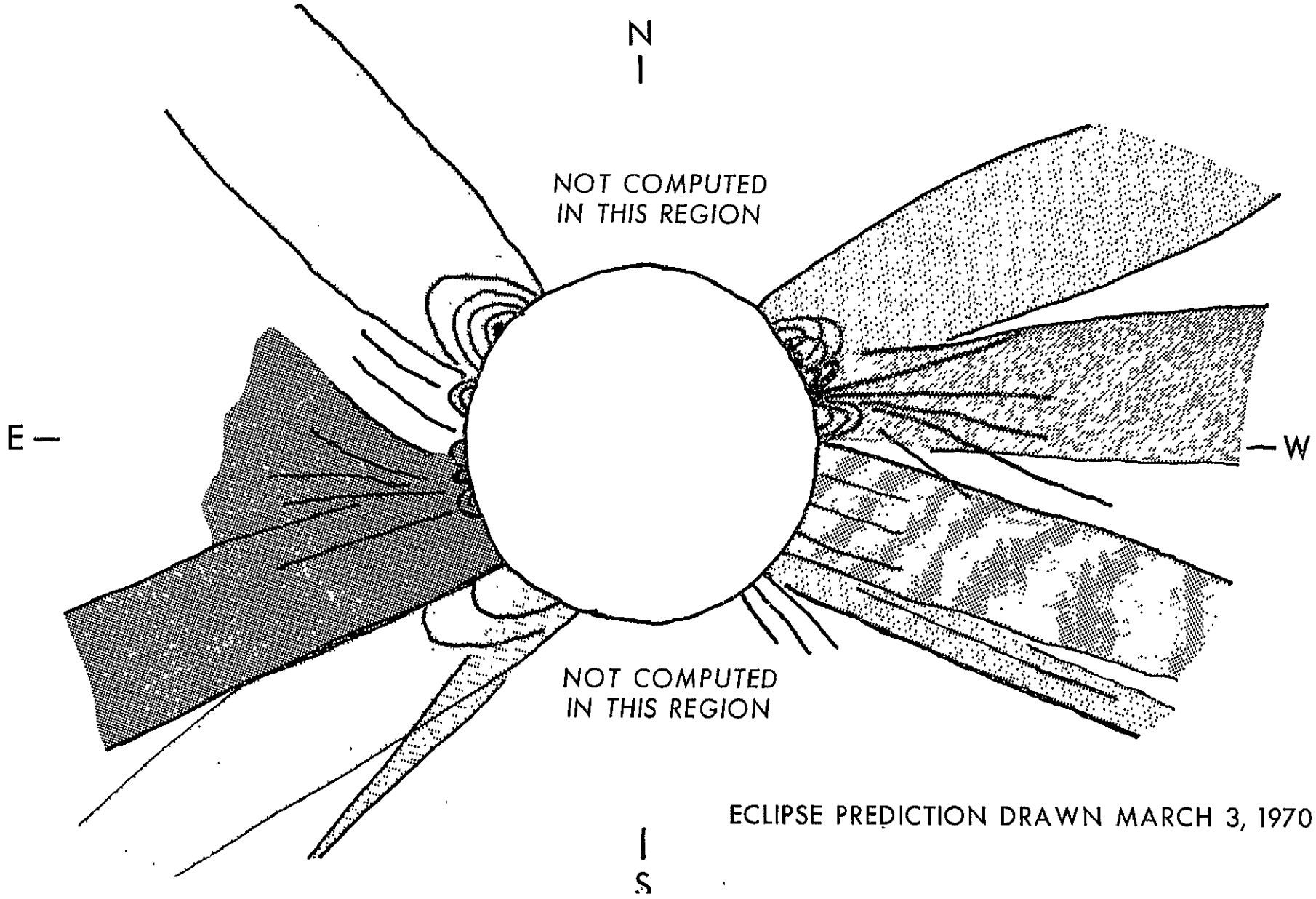
N
NOT COMPUTED
IN THIS REGION
E
W
NOT COMPUTED
IN THIS REGION
ECLIPSE PREDICTION DRAWN MARCH 3, 1970
S

FIGURE 13